

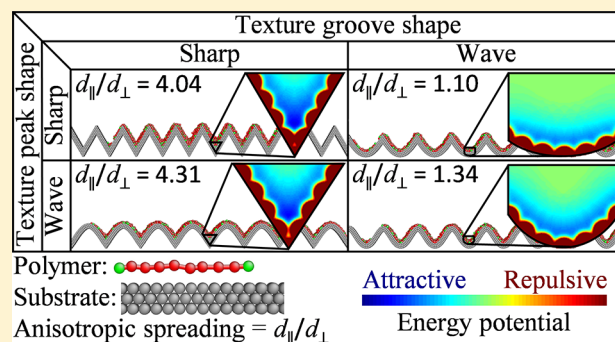
Polymer Spreading on Unidirectionally Nanotextured Substrates Using Molecular Dynamics

 Brooklyn A. Noble and Bart Raeymaekers*[✉]

Department of Mechanical Engineering, University of Utah, Salt Lake City, Utah 84112, United States

Supporting Information

ABSTRACT: A unidirectional nanotexture alters the wettability of a substrate and can be used to create patterned polymer films, tailored polymer coverage/reflow, or aligned polymer molecules. However, the physical mechanisms underlying polymer spreading on nanoscale textures are not well-understood, and competing theories exist to explain how texture peaks and grooves alter the wettability of a substrate. We use molecular dynamics to simulate polymer spreading on substrates with unidirectional nanoscale textures as a function of texture shape and size and compare to polymer spreading on a flat substrate. We show that the texture groove shape is the primary factor that modifies polymer spreading on unidirectionally nanotextured substrates because the texture groove shape determines the minimum potential energy of a substrate. At the texture groove, the energy potentials of several surfaces combine, which increases polymer attraction and drives spreading along the texture groove. A texture groove also acts as a sink that inhibits polymer spreading perpendicular to the texture. Texture peaks create energy barriers that inhibit polymer spreading perpendicular to the texture, but this is a secondary mechanism that does not significantly affect anisotropic spreading. This research unifies competing theories of anisotropic liquid spreading documented in the literature and aims to aid in the design of nanoscale textures and ultrathin liquid film systems.



INTRODUCTION

Understanding how liquid polymer interacts with a substrate on the nanoscale is of utmost importance for the design of many engineering applications. For instance, ultrathin (monolayer) liquid polymer films serve as protective lubricant coatings on hard disk drives¹ and antibiofouling coatings for medical devices,² and are an integral part of many nanoscale manufacturing processes,³ among many others. Despite their importance, controlling spreading and coverage of an ultrathin liquid polymer film on a substrate remains challenging because surface forces, as opposed to body forces like gravity, dominate on the nanoscale. To solve this problem, recent research has focused on altering substrate wettability through modification of substrate texture. Substrate texture increases lubricant reflow and reduces degradation of hard disk drive performance;⁴ a uniform nanotexture provides the most shear-tolerant, liquid-repellent, and nonfouling behavior compared to smooth or hierarchically textured substrates;⁵ and textured flange surfaces achieve an improved sealing effect.⁶ Consequently, understanding the physical mechanisms that underlie polymer film spreading in the presence of nanoscale texture features is necessary to enhance the performance of engineering applications that rely on ultrathin polymer films.

The ability to create anisotropic spreading in particular, which enables liquid spreading to occur in a user-specified direction, finds application in micro/nanofluidics,⁷ flexible

electronics,⁸ and drag reduction surfaces.⁷ Several research groups have shown both experimentally and numerically that unidirectionally textured substrates lead to anisotropic spreading, where liquids spread preferentially in the direction parallel to the texture.^{9–23} Anisotropic spreading on unidirectionally textured substrates is most commonly explained by texture peaks, which impose a mechanical barrier that effectively “pins” the three-phase (solid/liquid/gas) contact line of the spreading liquid, inhibiting spreading in the direction perpendicular to the texture.^{9–14,19–23} The texture peaks are often described as energetic barriers that oppose wetting,¹⁹ which Yong and Zhang²² attribute to a high local atomic density at texture peaks, based on the results of molecular dynamics (MD) simulations (texture height of 1.85–23.77 Å). The liquid may be confined by texture peaks in the perpendicular direction and “squeezed” in the parallel direction. Alternatively, the liquid may only be slowed by texture peaks, causing the contact line to advance in a stick-slip manner, pinning-depinning-repinning on subsequent texture peaks.^{10,11,14,19,20} Conversely, others propose that anisotropic spreading is caused by texture grooves that accelerate spreading along the direction parallel to the texture, i.e., along the grooves.^{9,10,15–18} Fischer et al.¹⁰ attribute

Received: April 9, 2019

Revised: May 28, 2019

Published: June 10, 2019

this accelerated spreading in part to capillary action inside the grooves, based on experiments with sinusoidal textures (height of 8 or 16 μm). In addition, Zhang et al.¹⁷ used Monte Carlo simulations and experiments (square-shaped textures with a height of 0.03–0.05 μm) to explain that an increased surface force exists inside a groove because it is surrounded by as many as three surfaces; i.e., a square groove is composed of a base and two side-walls. Moreover, some research groups recognize both texture peaks and texture grooves as inhibiting and accelerating mechanisms, respectively, but do not compare the strength of these mechanisms.^{9,10} In addition to competing theories regarding the physical mechanisms that cause anisotropic spreading, the texture parameters that affect anisotropic spreading on unidirectionally textured substrates are also studied because previous research has shown different effects. Many parameters such as texture groove depth,^{10,17} texture width,¹⁰ texture aspect ratio,^{19,21} and number of wetted texture peaks,¹³ among others⁷ have been proposed to affect anisotropic wetting.

Understanding the physical mechanisms underlying ultrathin liquid polymer film spreading on unidirectional nanotextured substrates is critical to designing complex ultrathin polymer systems. However, no publications seem to exist that provide a complete molecular-level explanation of how nanoscale textures affect polymer spreading and how texture peaks and texture grooves alter the wettability of a substrate. Thus, the objective of this work is to quantify polymer spreading on unidirectional nanotextured substrates and to provide a molecular-level explanation of polymer spreading on nanotextured substrates, as compared to a flat substrate, which we have studied previously.^{24–26} We perform MD simulations of liquid polymer spreading on rigid substrates with unidirectional nanotexture features of various shapes and sizes.

METHODS

We simulate liquid polymer spreading on textured substrates using a coarse-grained bead-spring (CGBS) model and the Large-Scale Atomic/Molecular Massively Parallel Simulator (LAMMPS).^{27,28} The CGBS model averages atomic interactions for computational efficiency yet preserves the essence of the molecular structure. We study Zdol, a linear random copolymer commonly used in many micro- and nanoscale devices, which has a backbone structure of $X-[(O-CF_2-CF_2)_p-(O-CF_2)_q]-O-X$ ($p/q \cong 2/3$) and terminates with a functional hydroxyl group ($X = CF_2-CH_2-OH$). The polymer molecules consist of $N = 10$ beads/molecule where the two terminating beads have an additional potential to simulate the functional hydroxyl group. The bead mass is 0.2 kg/mol; thus, the molecular weight is 2 kg/mol. The potential function interactions that define the system are similar to validated potentials used in previous research and are discussed in detail in the Supporting Information (SI).^{15,24–26,29–31} Gravity is negligible at this scale and, therefore, not included in our model.

Figure 1 shows 2D side views of a typical simulation of polymer spreading on a substrate with a sharp unidirectional nanotexture both (a) before and (b) after polymer spreading when the contact angle is nearly zero. The substrate consists of three rigid layers of beads. We use a quasi-random distribution to establish the initial position of the first bead of every polymer molecule and use a random walk approach to define the initial position of the additional beads belonging to each molecule, starting from the first bead. The quantity of polymer ($Q = 40,000$ beads) is constant for every simulation in this work. The polymer is free to move according to the microcanonical ensemble, and we hold the temperature constant at 300 K using a Langevin thermostat. We use a time step of 0.005τ (0.0313 ps) throughout all MD simulations. The polymer equilibrates within a 23 nm diameter cylinder for at least 500 000 time steps (approximately 15 ns), which

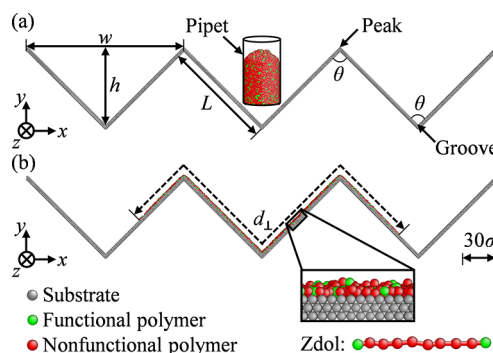


Figure 1. Side views of a typical molecular dynamics simulation of a liquid polymer (Zdol) both (a) before and (b) after spreading on a substrate with a sharp unidirectional nanotexture.

represents the pipet used in experiments to deposit a polymer droplet on a substrate. The cylindrical pipet is centered above a substrate texture groove. During equilibration, the potential energy of the system initially increases before approaching a constant value. We remove the cylinder after equilibration, and the polymer spreads on the substrate for approximately 6 500 000 time steps (approximately 200 ns). We have previously studied spreading kinetics for our model^{15,26} and have chosen simulation parameters (short polymer molecules without functional substrate groups) such that all simulations in this paper are described by the same spreading kinetics. The polymer spreading in our simulations is a dynamic process that results in a metastable configuration. Unless specifically stated otherwise, the polymer spreading is measured at the end of the simulation. We impose periodic boundary conditions around the simulation box, although the polymer does not cross any boundary during any simulation in this work.

We measure the final polymer spreading distance parallel to the texture $d_{||}$ and perpendicular to the texture d_{\perp} . Note that the polymer spreading distance perpendicular to the texture is the maximum distance the polymer spreads along the length of the substrate in the x - y plane (see Figure 1 for coordinate system), which is different from the apparent spreading distance obtained from a projection onto the x - z plane. We quantify polymer spreading parallel to the texture as the polymer spreading distance in the z -direction, i.e., along the grooves.

We evaluate the effect of the texture shape and size on polymer spreading. We define the aspect ratio of a texture as the width w to height h ratio. The length $15 \leq L \leq 250\sigma$ of a texture is defined as the distance from a peak to a groove, measured along the substrate. The shapes of texture peaks and grooves are either sharp with a defined angle $60^\circ \leq \theta \leq 180^\circ$ or rounded, i.e., a sinusoidal wave. A sharp texture with $\theta = 60^\circ$ is the smallest angle we consider because further reducing the angle results in overlapping substrate beads in the groove. A texture with $\theta = 180^\circ$ corresponds to a flat substrate. Figure 2 shows side views of six selected substrates that exemplify various texture shapes and sizes. Figure 2a and b shows textures with sharp peaks and grooves with defined angles of $\theta = 60^\circ$ and $\theta = 120^\circ$, respectively. Note that changing the texture angle also changes the aspect ratio as L remains constant. Figure 2c and d shows textures

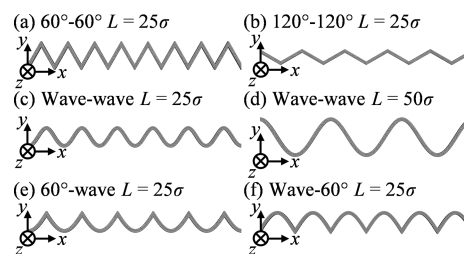


Figure 2. Side views of example textured substrates with various texture peak and groove shapes and sizes.

with wave peaks and grooves with lengths of $L = 25\sigma$ and $L = 50\sigma$, respectively. Changing the length does not change the aspect ratio. Figure 2e and f shows textures with a combination of sharp $\theta = 60^\circ$ and wave texture peaks and grooves.

RESULTS AND DISCUSSION

Figure 3 shows the polymer spreading distance both (a) parallel and (b) perpendicular to the substrate texture as a

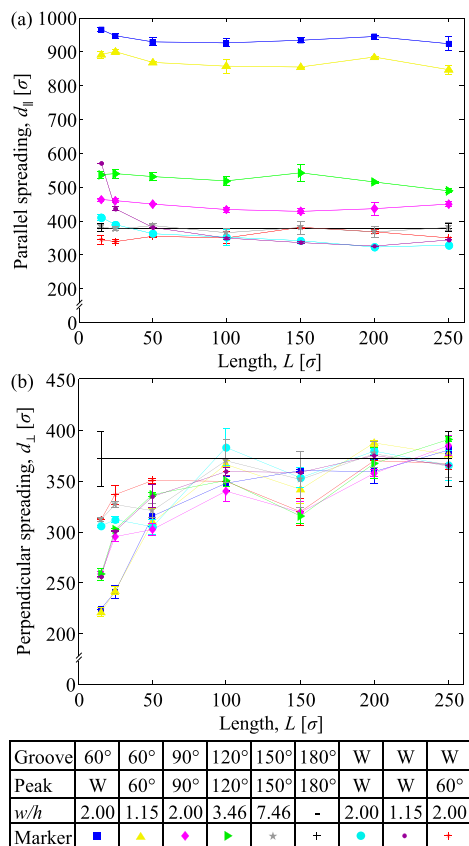


Figure 3. Polymer spreading (a) parallel and (b) perpendicular to substrate textures with various shapes as a function of the texture length.

function of the texture length. We show results for nine different substrate textures where we identify each peak shape, groove shape, and aspect ratio combination with a unique marker. Sinusoidal wave grooves and peaks are abbreviated as W. We repeat each simulation two times and report the average polymer spreading distance; error bars define the high and low results. Polymer spreading on a flat substrate ($\theta = 180^\circ$) is shown for reference, but a value for L is not applicable in this case.

From Figure 3a, we observe that d_{\parallel} is nearly independent of L . However, parallel spreading for a wave substrate with an aspect ratio $w/h = 1.15$ significantly increases with decreasing texture length. We also observe that textures with similar groove shapes yield similar parallel spreading results, despite different peak shapes. Very sharp grooves, e.g., $\theta = 60^\circ$, yield the most parallel spreading. Conversely, when a groove shape is nearly flat (e.g., $\theta = 150^\circ$ and wave grooves) polymer spreading parallel to the grooves is similar to that on a flat substrate. Thus, d_{\parallel} is determined by the shape of grooves such that sharp grooves promote spreading along the groove, independent of the texture peak shape. We also observe that

textures with the same aspect ratio can yield starkly different parallel spreading. For example, textures with $w/h = 2$ exhibit both the most (wave peaks with 60° grooves) and the least (60° peaks with wave grooves) parallel spreading. Thus, neither the texture aspect ratio nor the number of texture grooves/peaks the polymer encounters during spreading, which increases with decreasing L , seems to determine polymer spreading parallel to the texture.

From Figure 3b, we observe that the polymer typically spreads much less perpendicular to the texture than parallel to the texture, in agreement with previous reports.^{9,10,15–18} Similar to the case of Figure 3a, we observe that textures with the same aspect ratio can yield different d_{\perp} . Thus, the texture aspect ratio does not necessarily determine anisotropic spreading d_{\parallel}/d_{\perp} , in opposition to previous reports.^{19,21} We also observe that d_{\perp} decreases with decreasing L and that this is more pronounced for textures with sharp grooves, especially grooves with $\theta = 60^\circ$. For small L , d_{\perp} and d_{\parallel} are inversely related, indicating that the groove shape also determines d_{\perp} , independent of the texture peak shape. Spreading in the direction perpendicular to the groove decreases with decreasing L because the number of texture grooves/peaks the polymer encounters during spreading increases with decreasing L , in agreement with previous research.¹³ For textures with $L = 25\sigma$ and $d_{\perp} = 200\text{--}300\sigma$, the polymer encounters five grooves, and we observe that d_{\perp} is significantly smaller than the isotropic spreading observed on a flat substrate ($d_{\perp} = 372\sigma$). For the same textures but with $L = 50\sigma$, the polymer encounters three grooves ($d_{\perp} = 200\text{--}400\sigma$) and d_{\perp} increases compared to $L = 25\sigma$ but remains less than the spreading observed on a flat substrate. For the same textures but with $L = 100\sigma$, the polymer only encounters one groove ($d_{\perp} < 400\sigma$), above which the polymer is initially placed. Thus, the polymer overcomes zero grooves but two peaks, and we observe that the peaks do not inhibit spreading because d_{\perp} is similar to that obtained on a flat substrate. For large L , d_{\perp} for polymer spreading on textured and flat substrates are almost identical. When $L \geq 200\sigma$, the polymer only encounters a single groove and no peaks. The polymer spreads in a single groove and d_{\perp} is unaffected by the texture, as we have previously reported in detail.¹⁵ Figure S2 illustrates the number of grooves and peaks the polymer encounters during spreading on several example substrates. However, although perpendicular spreading depends on the number of grooves the polymer encounters, the groove shape is the dominant factor that determines anisotropic polymer spreading. For example, substrates with $L = 50\sigma$ all encounter three grooves but can yield different anisotropic spreading results, i.e., $d_{\parallel}/d_{\perp} = 2.87$ on average for grooves with $\theta = 60^\circ$ and $d_{\parallel}/d_{\perp} = 1.11$ on average for wave grooves.

We further explain the observations of Figure 3 by means of the potential energy associated with each texture groove and peak shape. Figure 4 shows 2D spatial potential energy maps at the peaks and grooves of five different substrates. The spatial potential energy maps display the superposition of the Lennard-Jones energy potential of each individual substrate bead, which represents the van der Waals interaction between a polymer bead and a substrate bead (see the SI). The dark red circular regions represent the positive (repulsive) energy of the substrate, i.e., where the substrate beads act as hard spheres. We also report the minimum potential energy in the grooves of each substrate. The locations of polymer bead centers are represented as magenta dots and overlay the potential energy

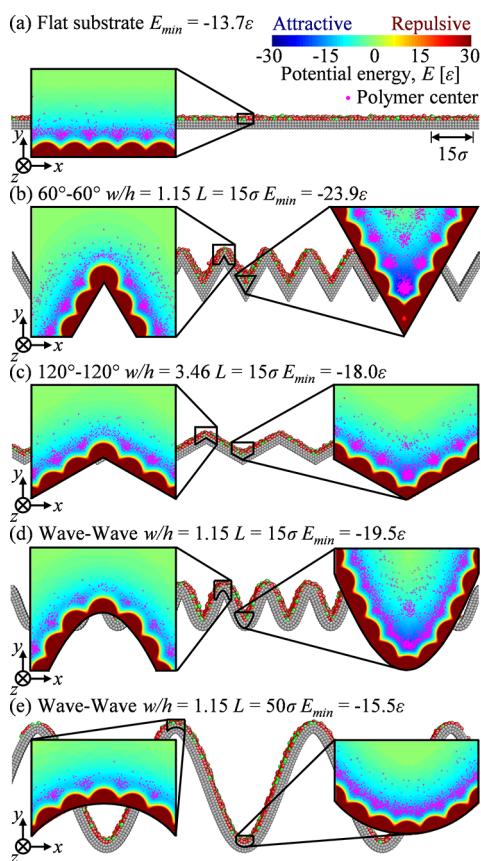


Figure 4. Two-dimensional spatial potential energy maps and polymer bead center locations at the peaks and grooves of substrates with different texture shapes and lengths.

maps. **Figure 4a** shows a flat substrate with a single potential energy map for reference.

From **Figure 4**, we observe dark blue regions in the grooves where the attractive energy potentials of multiple substrate beads superimpose. We also observe that polymer beads cluster in these regions to minimize their energy state. From **Figure 4b**, we observe that when $\theta = 60^\circ$, the minimum potential energy $E_{\min} = -23.9\epsilon$ is strong because substrate beads are closely packed where the groove forms a sharp edge. Thus, the surface force is maximum in a groove, which explains why spreading is promoted along sharp grooves, in agreement with previous research.^{15,17} Comparing **Figure 4a** and **e**, we observe that a flat substrate has a similar minimum potential energy ($E_{\min} = -13.7\epsilon$) to that of a wave texture with $L = 50\sigma$ ($E_{\min} = -15.5\epsilon$), and we observe similar polymer spreading on both of these substrates. Thus, a larger minimum potential energy promotes spreading parallel to the texture and appears to inhibit spreading perpendicular to the texture. Comparing **Figure 4b** and **c**, we observe that changing the angle of a substrate groove changes the minimum potential energy created by that groove, which explains why we observe significantly more spreading parallel to the texture for $\theta = 60^\circ$ compared to $\theta = 120^\circ$. Comparing **Figure 4d** and **e**, we observe that the minimum potential energy is significantly greater when $L = 15\sigma$ compared to $L = 50\sigma$ for a sinusoidal wave texture with the same aspect ratio. Because the shape of a groove with a defined angle does not change with L , the minimum potential energy is the same for all substrates with a specific angle, independent of L . This is not the case for wave grooves

because the shape of the groove, and thus the superposition of the energy potentials, varies with L . Hence, parallel spreading observed along wave grooves increases for decreasing L but remains constant along grooves with a defined angle.

From **Figure 4**, we also observe that the potential energy increases at texture peaks such that the potential energy approaches zero. Additionally, we note that the polymer quantity locally decreases at texture peaks because the attractive energy potentials of fewer substrate beads superimpose, and polymer molecules avoid these regions to minimize their energy state. **Figure S3** shows local polymer quantity maps that further demonstrate how polymer tends to dewet texture peaks. This finding is in opposition to Yong and Zhang²² who suggested that peaks oppose wetting because of high local atomic density.

Because we observe that a greater minimum potential energy promotes spreading parallel to the texture but inhibits spreading perpendicular to the texture, we more closely investigate how spreading in each direction and the minimum potential energy compare. **Figure 5a** shows polymer spreading

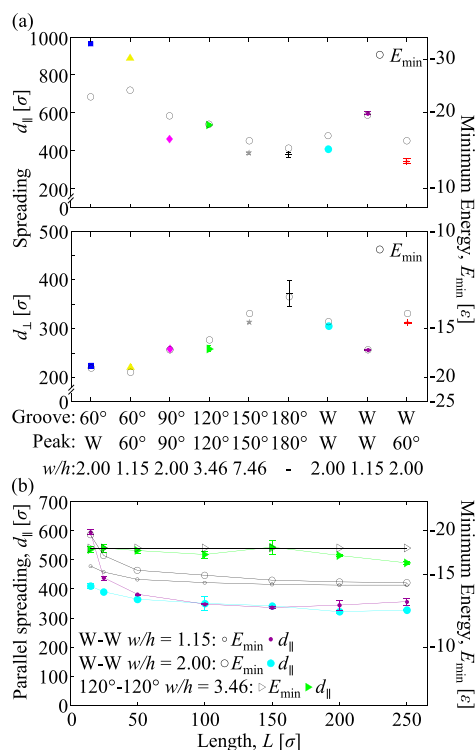


Figure 5. (a) Minimum potential energy and polymer spreading parallel and perpendicular to the texture as a function of texture shape for $L = 15\sigma$. (b) Minimum potential energy and polymer spreading parallel to the texture as a function of the texture length for three selected textures.

parallel and perpendicular to the texture and the minimum potential energy (black circle markers) for each peak shape, groove shape, and aspect ratio combination with $L = 15\sigma$. Sinusoidal wave grooves and peaks are abbreviated as W. **Figure 5b** shows the polymer spreading distance parallel to the texture and the minimum potential energy (black hollow markers) as a function of L for three selected textures.

From **Figure 5a**, we indeed observe that parallel spreading correlates to the minimum potential energy and that perpendicular spreading inversely correlates to the minimum

potential energy. Thus, the shape of texture grooves determines the minimum potential energy, which in turn determines the polymer spreading distance parallel and perpendicular to the texture. Figure S4 shows polymer spreading parallel and perpendicular to the texture versus the texture minimum energy to further illustrate their correlation. From Figure 5b, we observe that polymer spreading parallel to the texture also correlates to the minimum potential energy for different substrate texture lengths. For a wave texture with an aspect ratio $w/h = 1.15$, we observe that parallel spreading and the minimum potential energy significantly increase with decreasing texture length. This also occurs for a wave texture with an aspect ratio $w/h = 2.00$ but is less pronounced. Therefore, the minimum potential energy of sinusoidal wave substrates, and thus the polymer spreading distance parallel to the texture, is affected by L , and this effect increases with decreasing aspect ratio. However, the minimum potential energy is independent of L for $\theta = 120^\circ$ because the shape of a groove with a defined angle does not change with L .

We further explain how spreading perpendicular to the texture is inhibited by examining the polymer spreading kinetics on two different textures. Figure 6 shows spreading

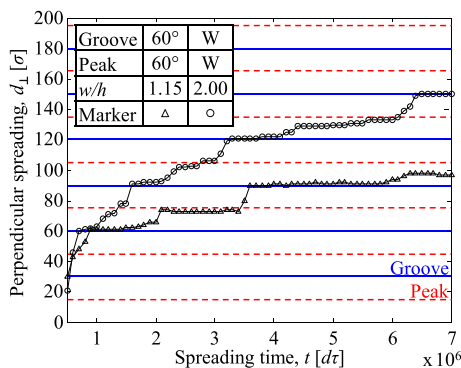


Figure 6. Polymer spreading perpendicular to the texture in one direction as a function of time for two example simulations. Red dashed lines and solid blue lines correspond to the locations of texture peak and groove structures, respectively.

perpendicular to the texture in one direction, measured from the center of the cylindrical pipet that initially confines the polymer, as a function of time for two different simulations: $\theta = 60^\circ$ peaks and grooves and sinusoidal wave peaks and grooves. Dashed red lines indicate the perpendicular polymer spreading distance that corresponds to the locations of substrate texture peaks, and solid blue lines indicate the perpendicular polymer spreading distance that corresponds to the locations of substrate texture grooves.

From Figure 6, we observe that spreading is nonlinear with time; steps form such that d_\perp is constant as a function of time when the polymer spreading front reaches texture grooves and peaks. Thus, in agreement with Kubiak and Mathia⁹ and Fischer et al.,¹⁰ both peaks and grooves modify spreading, and we observe the pinning-depinning-repinning spreading mechanism previously described.^{10,11,14,19,20} We also observe that the sharp $\theta = 60^\circ$ substrate grooves and peaks inhibit perpendicular spreading longer than the sinusoidal wave grooves and peaks.

Because we observe from Figure 3 that polymer spreading is dependent on the groove shape and independent of the peak shape, we conclude that the energy minimum created in a

groove is the main factor that determines anisotropic spreading. Grooves act as sinks that slow spreading perpendicular to the grooves because polymer is pulled along the grooves. Peaks can act to “pin” the polymer and inhibit spreading perpendicular to the grooves in agreement with previous research,^{9–14,19–23} but this is a secondary mechanism that mainly affects spreading kinetics but does not significantly affect anisotropic spreading. By comparing two textures both with sinusoidal wave peaks, $w/h = 2.00$, and $L = 15\sigma$ but one substrate with $\theta = 60^\circ$ grooves and the other with sinusoidal wave grooves, we observe that d_\parallel increases by 136% and d_\perp decreases by 27% when spreading on grooves with $\theta = 60^\circ$. Hence, by only changing the groove shape from a sinusoidal wave to $\theta = 60^\circ$, the anisotropic spreading increases from 1.34 to 4.31 (222% increase). Alternatively, we compare two textures both with sinusoidal wave grooves, $w/h = 2.00$ and $L = 15\sigma$ but one substrate with $\theta = 60^\circ$ peaks and the other with sinusoidal wave peaks. We observe that d_\parallel increases by 19% and d_\perp decreases by 2% when spreading on sinusoidal wave peaks. Thus, the anisotropic spreading is effectively unaltered (22% increase).

CONCLUSIONS

Groove shape determines anisotropic polymer spreading on unidirectional nanotextured substrates. Spreading both parallel and perpendicular to a unidirectional nanotexture is dependent on the texture groove shape because the texture groove shape affects the minimum potential energy of the substrate. Polymer spreading anisotropy increases with increasing aspect ratio for sharp grooves, but this is not the underlying mechanism as textures with the same aspect ratio can yield starkly different spreading results. For sharp texture grooves, the energy potentials of a greater number of surfaces combine at the same location to strongly attract polymer to spread along the texture grooves, also acting as a sink that inhibits polymer spreading perpendicular to the texture groove; this is the main mechanism that both promotes parallel spreading and inhibits perpendicular spreading on a unidirectional nanotexture. Texture peaks create an energy barrier that can confine the spreading liquid in the direction perpendicular to the substrate texture, but this is a secondary mechanism that affects spreading kinetics but does not greatly affect anisotropic spreading. For applications with textured substrates where controlled wetting is desired, sharp grooves can be exploited. However, in order to create uniform monolayer polymer coverage on a substrate, the presence of sharp peaks should be avoided as polymer dewets sharp peaks.

ASSOCIATED CONTENT

Supporting Information

The Supporting Information is available free of charge on the ACS Publications website at DOI: 10.1021/acs.langmuir.9b01050.

Potential functional interactions; number of groove and peaks encountered; local polymer quantity; spreading and minimum potential energy correlation; (PDF)

AUTHOR INFORMATION

Corresponding Author

*Mailing address: 1495 E. 1000 S., 1550 MEK, Salt Lake City, UT 84112; Telephone: 801-581-6441. E-mail: bart.raeymaekers@utah.edu.

ORCID 

Bart Raeymaekers: 0000-0001-5902-3782

Notes

The authors declare no competing financial interest.

■ ACKNOWLEDGMENTS

This work used the Extreme Science and Engineering Discovery Environment (XSEDE) Comet at the San Diego Supercomputer Center through allocation MSS150011, which is supported by the National Science Foundation Grant Number ACI-1053575. The support and resources from the Center for High Performance Computing at the University of Utah are gratefully acknowledged. B.N. also gratefully acknowledges the Department of Energy Stewardship Science Graduate Fellowship program support, provided under Grant Number DE-NA0003864.

■ REFERENCES

- (1) Marchon, B. Lubricant Design Attributes for Subnanometer Head-Disk Clearance. *IEEE Trans. Magn.* **2009**, *45* (2), 872–876.
- (2) Maitz, M. F. Applications of Synthetic Polymers in Clinical Medicine. *Biosurface and Biotribology* **2015**, *1* (3), 161–176.
- (3) *Advances in Polymer Materials and Technology*; Srinivasan, A., Bandyopadhyay, S., Eds.; CRC Press, 2016; DOI: 10.1201/9781315371054.
- (4) Tan, A. H.; Cheng, S. W. A Novel Textured Design for Hard Disk Tribology Improvement. *Tribol. Int.* **2006**, *39* (6), 506–511.
- (5) Kim, P.; Kreder, M. J.; Alvarenga, J.; Aizenberg, J. Hierarchical or Not? Effect of the Length Scale and Hierarchy of the Surface Roughness on Omniphobicity of Lubricant-Infused Substrates. *Nano Lett.* **2013**, *13* (4), 1793–1799.
- (6) Liang, Y.; Shu, L.; Natsu, W.; He, F. Anisotropic Wetting Characteristics versus Roughness on Machined Surfaces of Hydrophilic and Hydrophobic Materials. *Appl. Surf. Sci.* **2015**, *331*, 41–49.
- (7) Xia, D.; Johnson, L. M.; López, G. P. Anisotropic Wetting Surfaces with One-Dimensional and Directional Structures: Fabrication Approaches, Wetting Properties and Potential Applications. *Adv. Mater.* **2012**, *24* (10), 1287–1302.
- (8) Fukuzawa, K.; Deguchi, T.; Yamawaki, Y.; Itoh, S.; Muramatsu, T.; Zhang, H. Control of Wettability of Molecularly Thin Liquid Films by Nanostructures. *Langmuir* **2008**, *24* (6), 2921–2928.
- (9) Kubiak, K. J.; Mathia, T. G. Anisotropic Wetting of Hydrophobic and Hydrophilic Surfaces - Modelling by Lattice Boltzmann Method. *Procedia Eng.* **2014**, *79* (1st ICM), 45–48.
- (10) Fischer, G.; Bigerelle, M.; Kubiak, K. J.; Mathia, T. G.; Khatir, Z.; Anselme, K. Wetting of Anisotropic Sinusoidal Surfaces—experimental and Numerical Study of Directional Spreading. *Surf. Topogr.: Metrol. Prop.* **2014**, *2* (4), 044003.
- (11) Vaikuntanathan, V.; Sivakumar, D. Directional Motion of Impacting Drops on Dual-Textured Surfaces. *Phys. Rev. E* **2012**, *86* (3), 036315.
- (12) Dokowicz, M.; Nowicki, W. Morphological Transitions of Droplets Wetting a Series of Triangular Grooves. *Langmuir* **2016**, *32* (28), 7259–7264.
- (13) Vaikuntanathan, V.; Sivakumar, D. Maximum Spreading of Liquid Drops Impacting on Groove-Textured Surfaces: Effect of Surface Texture. *Langmuir* **2016**, *32* (10), 2399–2409.
- (14) Semperebon, C.; Herrmann, C.; Liu, B.; Seemann, R.; Brinkmann, M. Shape Evolution of Droplets Growing on Linear Microgrooves. *Langmuir* **2018**, *34*, 10498–10511.
- (15) Noble, B. A.; Raeymaekers, B. Polymer Spreading on Substrates with Nanoscale Grooves Using Molecular Dynamics. *Nanotechnology* **2019**, *30* (9), 095701.
- (16) Zhang, H.; Mitsuya, Y.; Yamada, M.; Fukuzawa, K. Measurement of Spreading Characteristics of Molecularly Thin Lubricant Films over Grooved Solid Surfaces Based on Diffraction Simulations. *Microsyst. Technol.* **2007**, *13* (8–10), 895–904.
- (17) Zhang, H.; Mitsuya, Y.; Yamada, M. Spreading Characteristics of Molecularly Thin Lubricant on Surfaces with Groove-Shaped Textures: Monte Carlo Simulation and Measurement Using PFPE Film. *J. Tribol.* **2002**, *124* (3), 575–583.
- (18) Zhang, H.; Mitsuya, Y.; Yamada, M. Spreading Characteristics of Molecularly Thin Lubricant on Surfaces with Groove-Shaped Textures: Effects of Molecular Weight and End-Group Functionality. *J. Tribol.* **2003**, *125* (2), 350–357.
- (19) Chung, J. Y.; Youngblood, J. P.; Stafford, C. M. Anisotropic Wetting on Tunable Micro-Wrinkled Surfaces. *Soft Matter* **2007**, *3* (9), 1163–1169.
- (20) Hirvi, J. T.; Pakkanen, T. A. Wetting of Nanogrooved Polymer Surfaces. *Langmuir* **2007**, *23* (14), 7724–7729.
- (21) Kusumaatmaja, H.; Vrancken, R. J.; Bastiaansen, C. W. M.; Yeomans, J. M. Anisotropic Drop Morphologies on Corrugated Surfaces. *Langmuir* **2008**, *24* (14), 7299–7308.
- (22) Yong, X.; Zhang, L. T. Nanoscale Wetting on Groove-Patterned Surfaces. *Langmuir* **2009**, *25* (9), 5045–5053.
- (23) Rahman, M. A.; Jacobi, A. M. Wetting Behavior and Drainage of Water Droplets on Microgrooved Brass Surfaces. *Langmuir* **2012**, *28* (37), 13441–13451.
- (24) Noble, B.; Ovcharenko, A.; Raeymaekers, B. Quantifying Lubricant Droplet Spreading on a Flat Substrate Using Molecular Dynamics. *Appl. Phys. Lett.* **2014**, *105* (15), 151601.
- (25) Noble, B. A.; Ovcharenko, A.; Raeymaekers, B. Terraced Spreading of Nanometer-Thin Lubricant Using Molecular Dynamics. *Polymer* **2016**, *84*, 286–292.
- (26) Noble, B. A.; Mate, C. M.; Raeymaekers, B. Spreading Kinetics of Ultrathin Liquid Films Using Molecular Dynamics. *Langmuir* **2017**, *33* (14), 3476–3483.
- (27) Plimpton, S. Fast Parallel Algorithms for Short-Range Molecular Dynamics. *J. Comput. Phys.* **1995**, *117* (1), 1–19.
- (28) Towns, J.; Cockerill, T.; Dahan, M.; Foster, I.; Gaither, K.; Grimshaw, A.; Hazelwood, V.; Lathrop, S.; Lifka, D.; Peterson, G. D.; et al. XSEDE: Accelerating Scientific Discovery. *Comput. Sci. Eng.* **2014**, *16* (5), 62–74.
- (29) Guo, Q.; Izumisawa, S.; Phillips, D. M.; Jhon, M. S. Surface Morphology and Molecular Conformation for Ultrathin Lubricant Films with Functional End Groups. *J. Appl. Phys.* **2003**, *93*, 8707–8709.
- (30) Hsia, Y. T.; Guo, Q.; Izumisawa, S.; Jhon, M. S. The Dynamic Behavior of Ultrathin Lubricant Films. *Microsyst. Technol.* **2005**, *11* (8–10), 881–886.
- (31) Chen, H.; Guo, Q.; Jhon, M. S. Effects of Molecular Structure on the Conformation and Dynamics of Perfluoropolyether Nanofilms. *IEEE Trans. Magn.* **2007**, *43* (6), 2247–2249.